

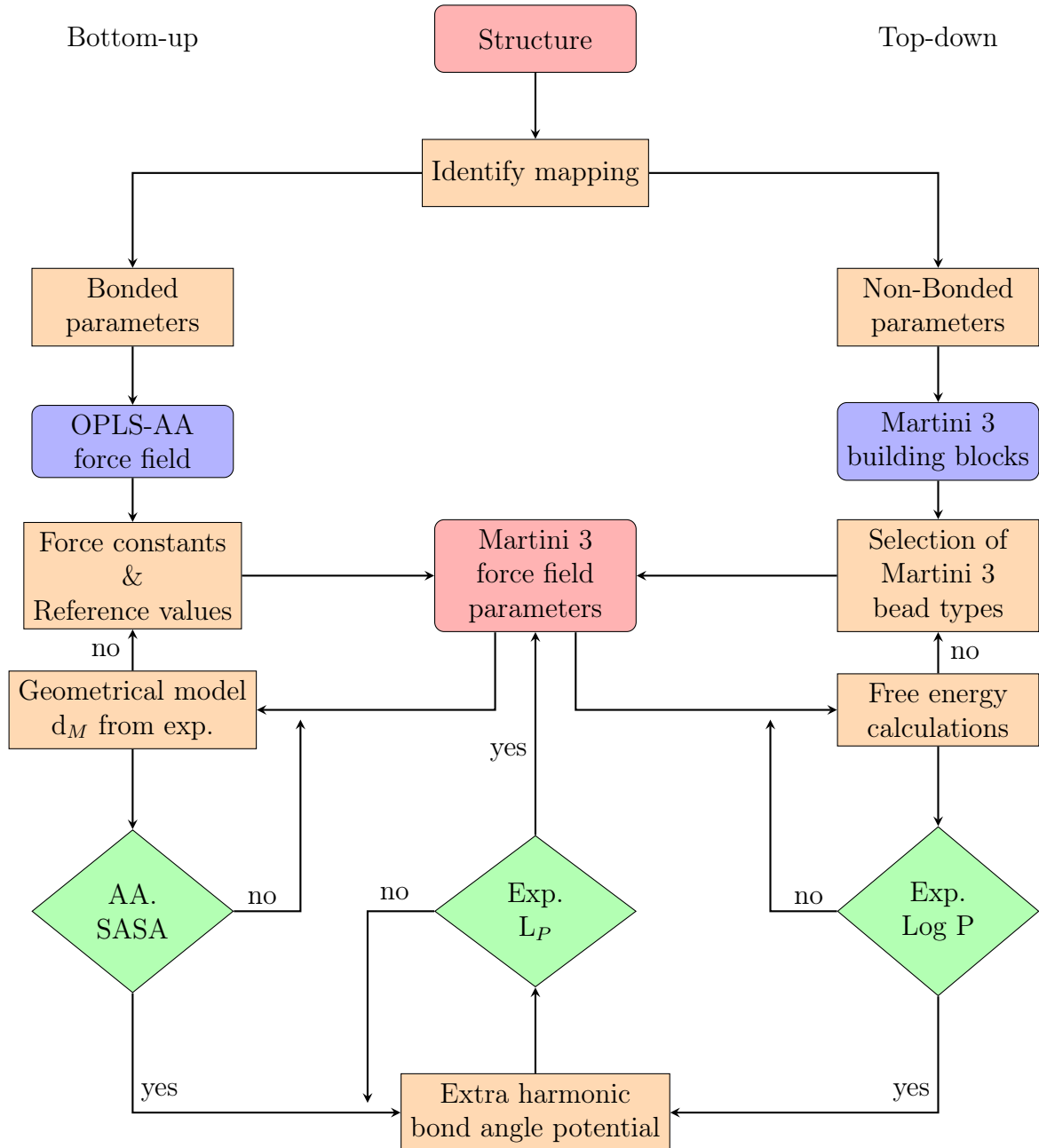
Supporting information for: Martini 3 Coarse-Grained Force Field for Poly(*para*-phenylene ethynylene)s

Matthias Brosz,^{ab} Nicholas Micherlarakis,^a Uwe H. F. Bunz,^c
Camilo Aponte-Santamaría^a and Frauke Gräter^{*ab}

^a Molecular Biomechanics Group, Heidelberg Institute for Theoretical Studies,
Am Schlosswolfsbrunnenweg 35, 69118 Heidelberg, Germany. E-mail: frauke.graeter@h-its.org

^b Interdisciplinary Center for Scientific Computing, Heidelberg University, Im Neuenheimer Feld 205,
69120 Heidelberg, Germany.

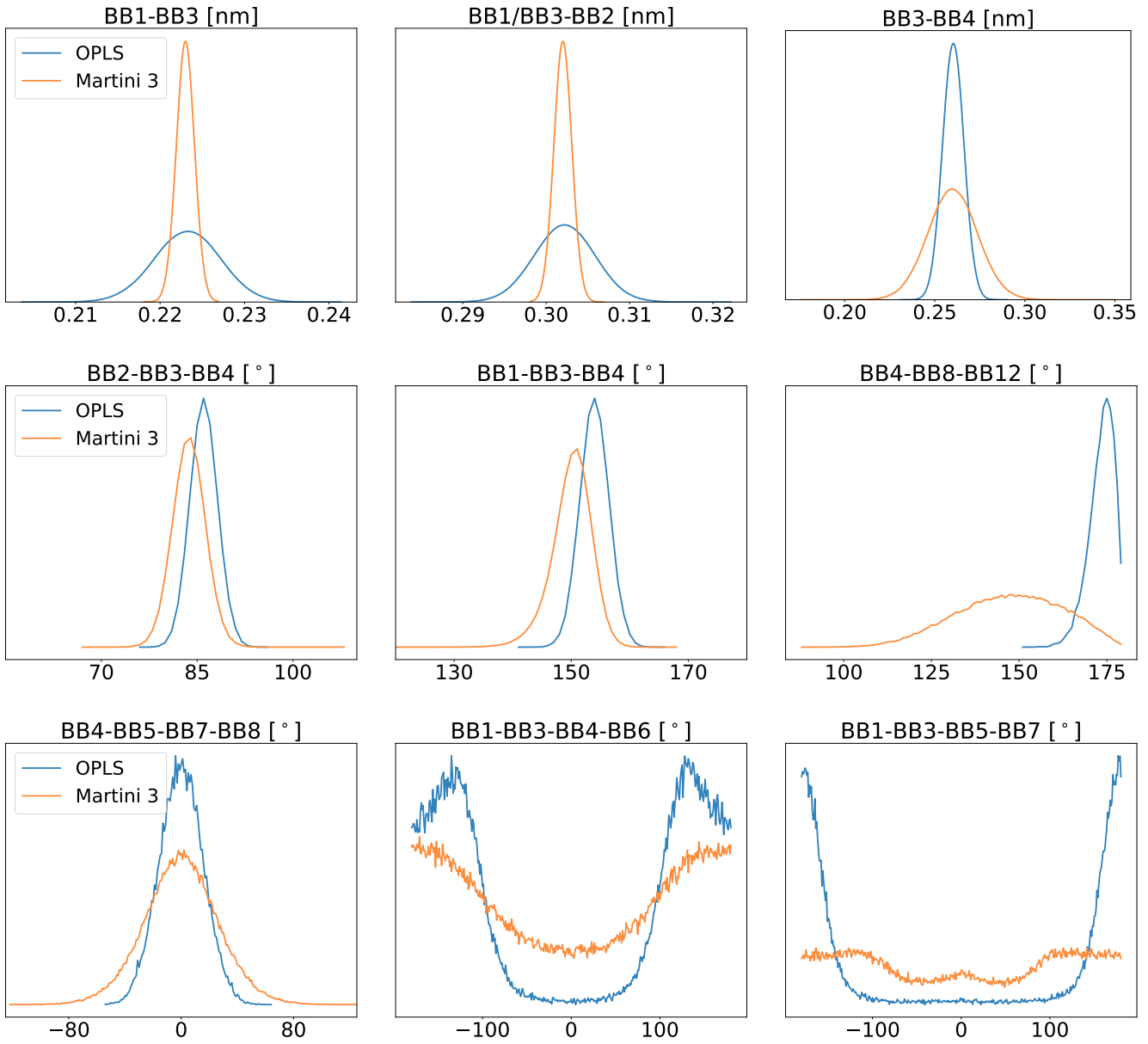
^c Institute of Organic Chemistry, Heidelberg University, Im Neuenheimer Feld 270, 69120 Heidelberg,
Germany.



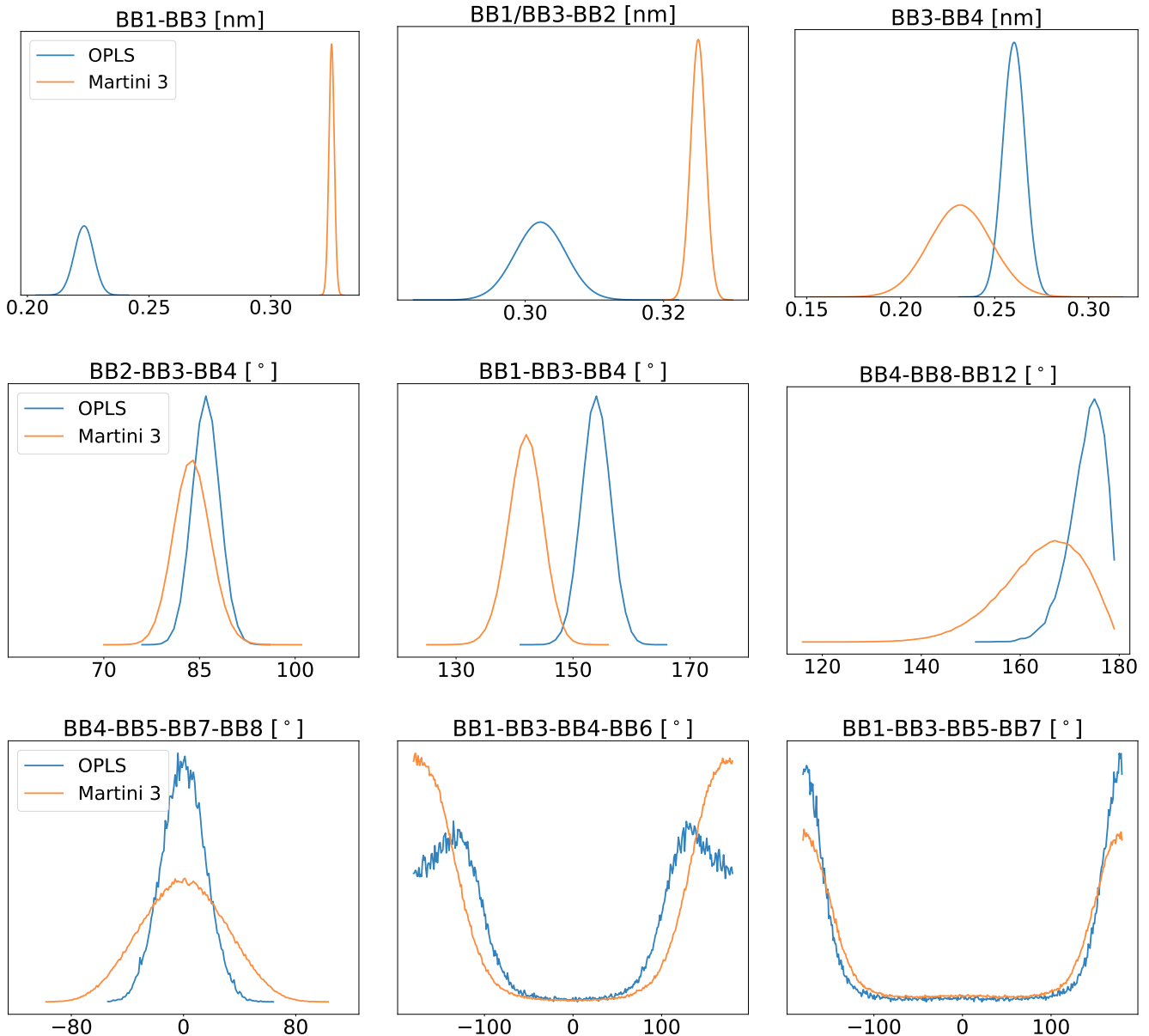
Supporting Figure 1 – Flow chart for coarse-graining PPEs with Martini 3. The purple boxes represent external information from the OPLS-AA force field or the Martini 3 building block data base. The orange boxes represent individual steps performed to develop the Martini 3 force field for PPEs. The green rhombuses are decision boxes representing properties for matching the CG model to AA simulations or experiments. As long as the properties do not agree (decision arrows equal 'no'), we adjusted the Martini 3 force field parameters in an iterative way. For the bonded parameters (*left*), we used a geometrical model to update the reference values of the force field. For the non-bonded ones (*right*), we adjusted the selected bead types. Once both properties agree (decision arrows turn to 'yes'), we introduced an additional harmonic bond angle potential to match the persistence length L_P of the Martini 3 coarse-grained model to experiments. By adjusting the force constant of the extra harmonic bond angle potential, we tailored the mechanical bending stiffness of a single polymer chain to experimental data (decision arrow turns to 'yes') to obtain the final Martini 3 force field parameter set.

Supporting Table 1 – Validation and tuning properties for the PPE Martini 3 model. To fine tune the Martini 3 force field parameters, we used three different kinds of single chain properties, namely the partition coefficient, the persistence length and the solvent accessible surface area (SASA). For validation purposes, we compared the packing in bundles and mid-size bulk systems to experiments or atomistic reference simulations. For the former, we focused on the radial and axial displacement of chains within the bundle of PPEs, given by the π stacking and side-by-side sliding, respectively, and for the latter on the bulk density and spatial correlations of mid-size polymer networks.

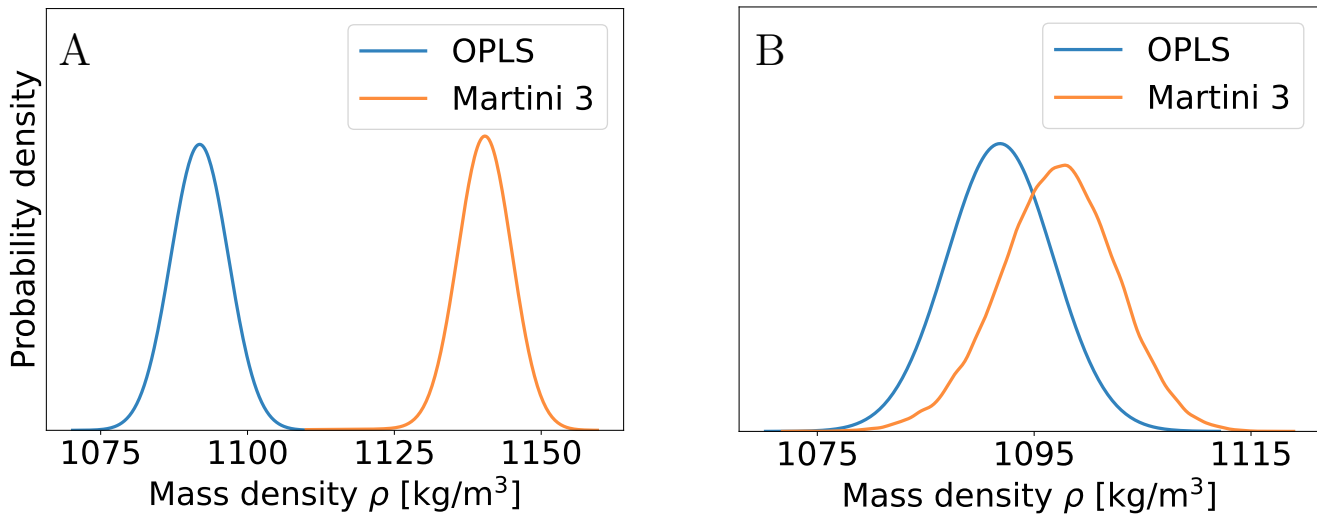
Property	Martini 3	OPLS-AA	Experimental
Properties to tune the model			
Log P_{Oct-H_2O} [-]	4.82 ± 0.02	-	4.78 ^[1]
Persistence length L_P [nm]	14.7 ± 1.3	-	$13.5 - 16.0$ ^[2]
SASA [nm 2]	13.20	13.22	-
Properties to validate the model			
Bulk density [kg m $^{-3}$]	1098	1092	-
π stacking [nm]	~ 0.5	~ 0.5	~ 0.4 ^[3,4]
Side-by-side sliding peak [nm]	0	± 0.13	-
Radial distribution function [nm]	0.57	0.58	-



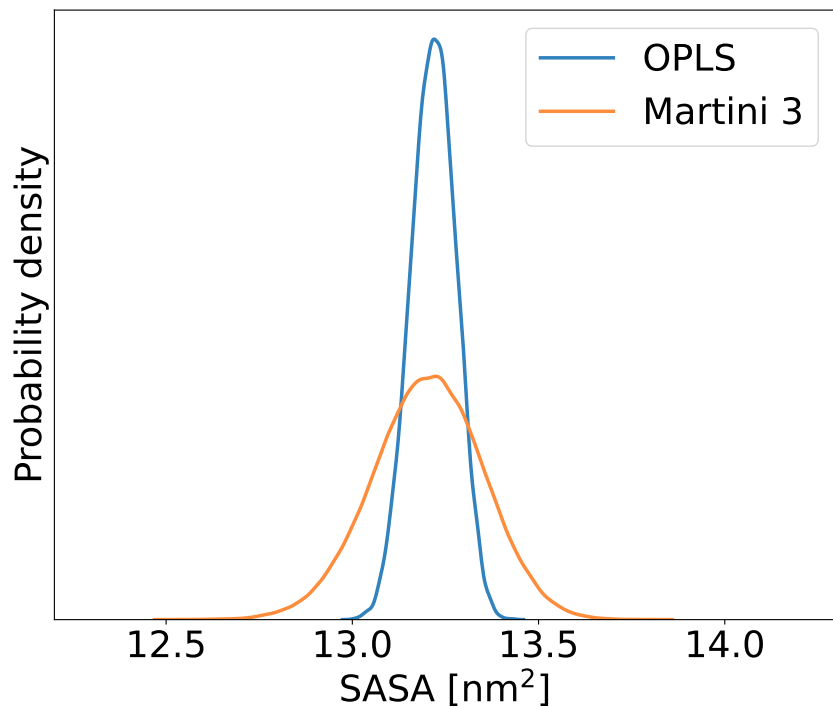
Supporting Figure 2 – Matching probability densities based on center-of-geometry mapping. Probability densities for bond length (*top*), bond angle (*middle*) and dihedral angle potentials (*bottom*) obtained from center-of-geometry mapping. Good agreement for probability densities from Martini 3 and mapped AA simulations. However, probability densities for dihedral angles were wider than the AA ones.



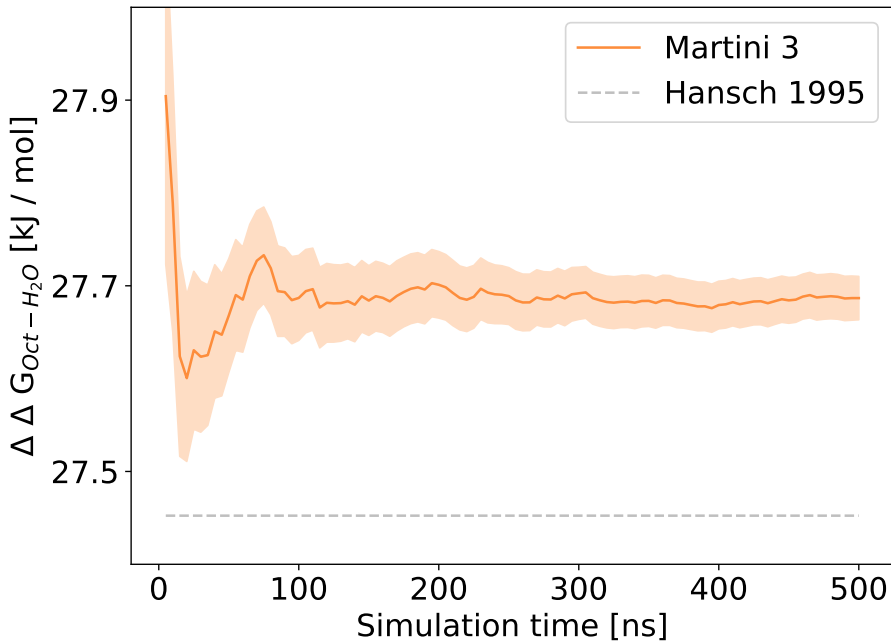
Supporting Figure 3 – Comparing probability densities obtained from geometrical modeling. Probability densities for bond length (*top*), bond angle (*middle*) and dihedral angle potentials (*bottom*) partly deviated from the mapped AA ones. The extra harmonic bond angle potential between three adjacent triple bond beads reduced the width of the dihedral angle probability densities.



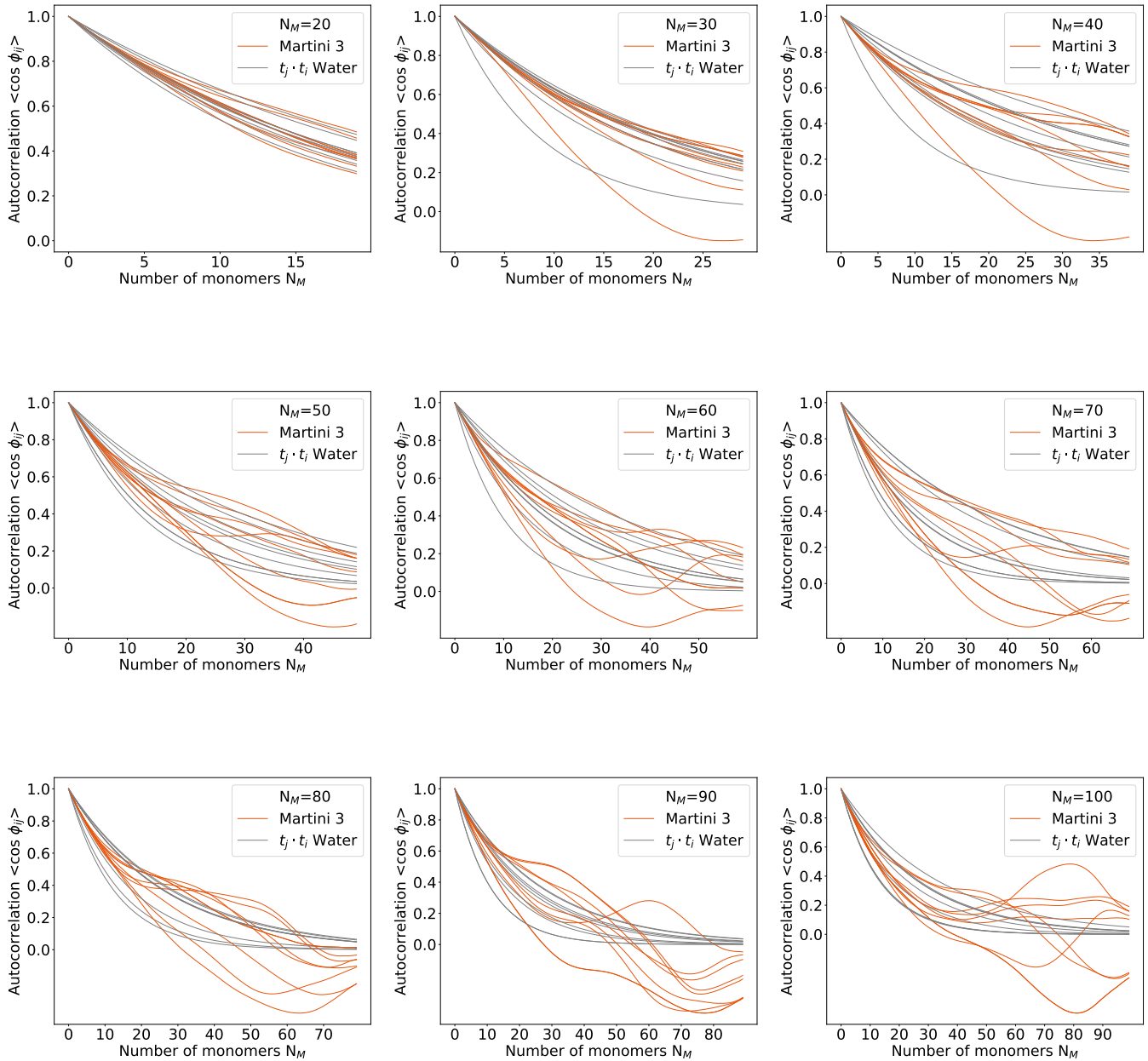
Supporting Figure 4 – Bulk density for center-of-geometry mapping and geometrical modeling. A Mass density for a bulk system containing 300 PPEs with lengths of four monomers. Mass density obtained from the center-of-geometry based mapping scheme (Fig. S2). B Mass density obtained from the geometrical modeling scheme (Fig. S3). The geometrical model reduced the difference for the bulk density between reference AA and Martini 3 simulations to less than 1% .



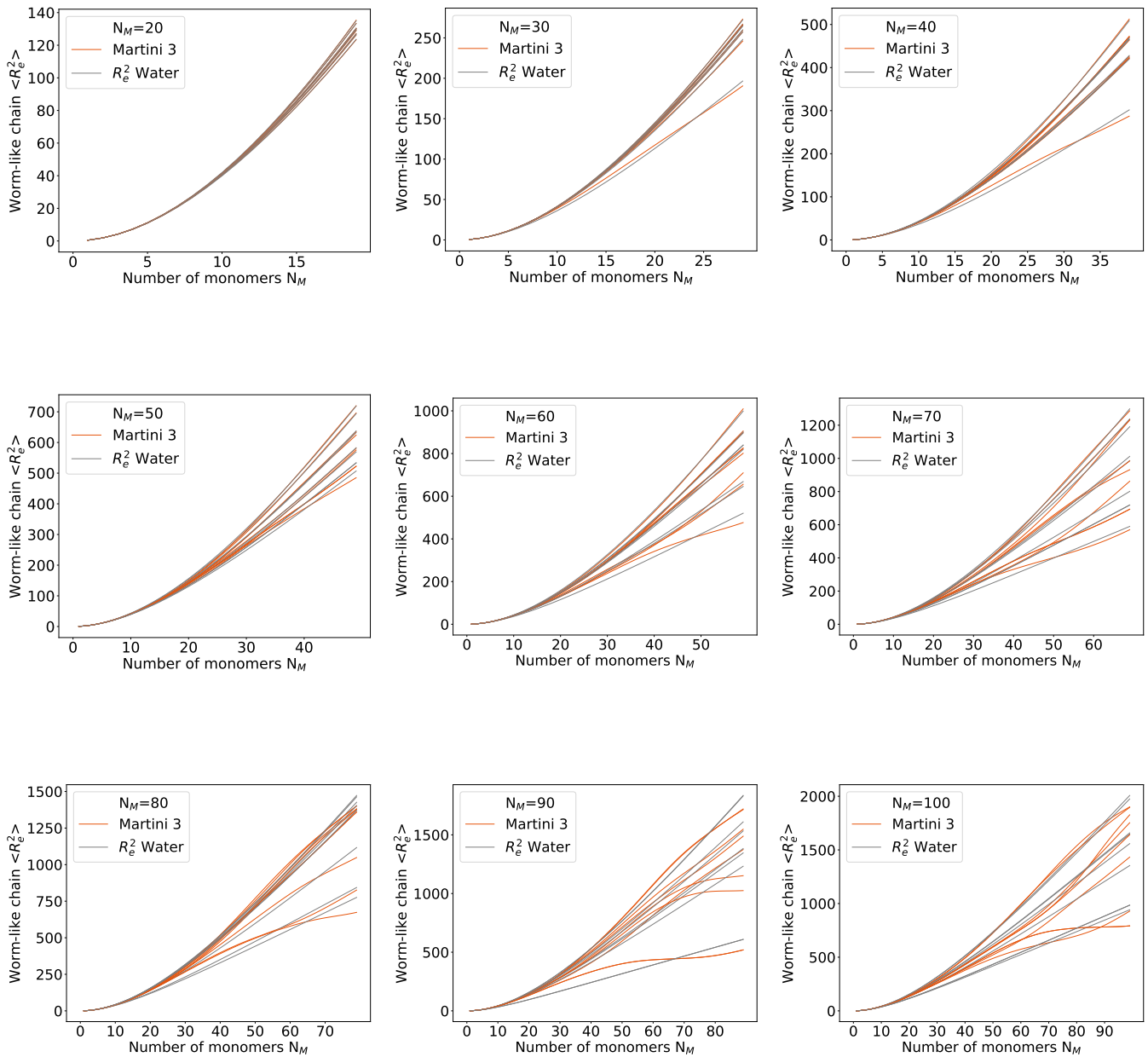
Supporting Figure 5 – Parameterising the geometrical model. We tuned the geometrical model, in particular the side length of the regular triangles d_{BT} , through matching the solvent accessible surface area (SASA) of a single four monomer long PPE chain from Martini 3 to AA simulations, to take the π conjugated backbone into account.



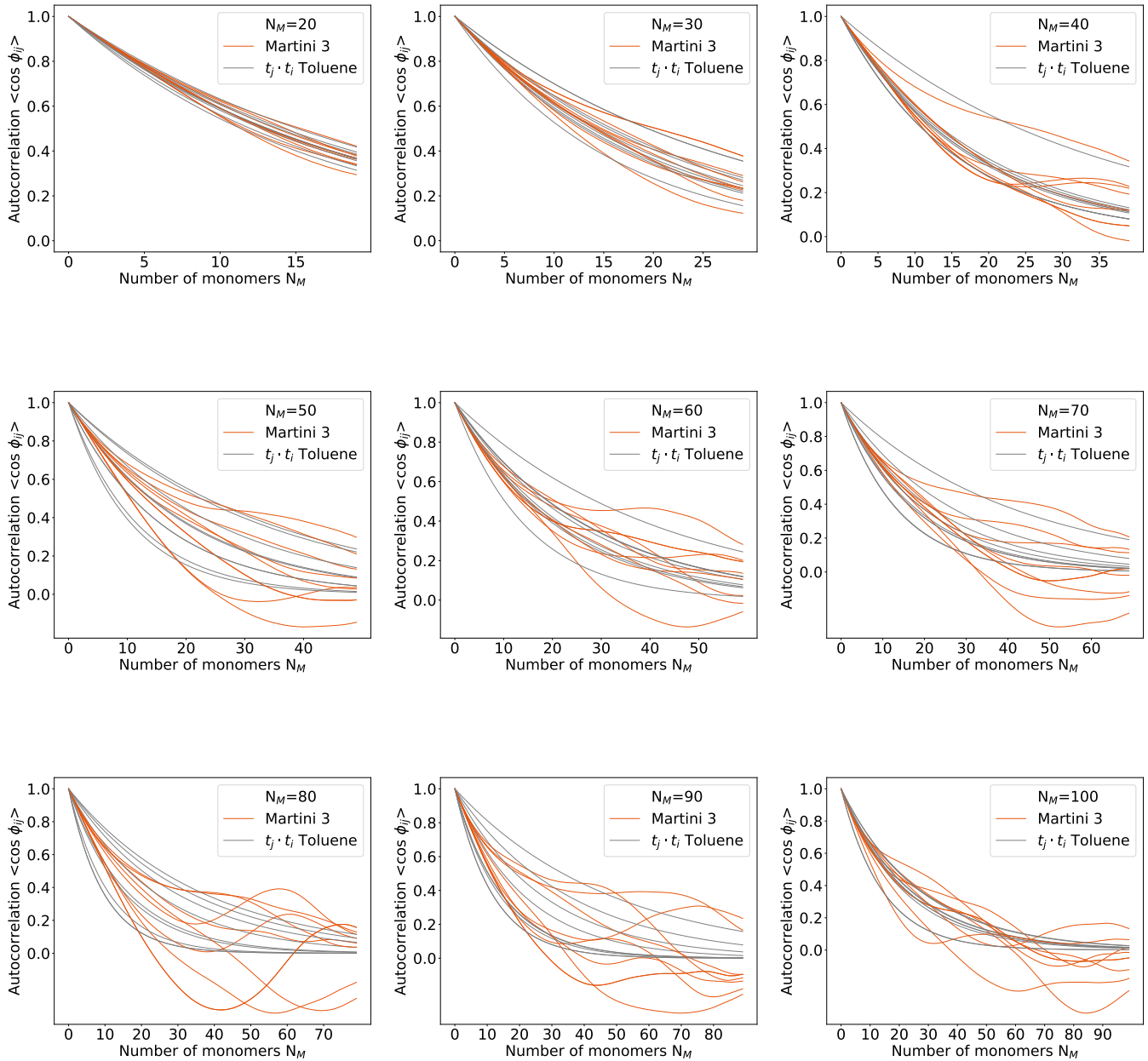
Supporting Figure 6 – Convergence analysis for the partitioning free energy of Tolane. The backward block average together with the absolute error for Tolane's free energy of transfer in an octanol-/water system obtained from umbrella sampling. For convergence analysis, we performed backward block averaging with a 5 ns step size, and for error estimation purposes, Bayesian bootstrapping. Based on a cumulative 6 microseconds simulation, we estimated the partitioning free energy $\Delta\Delta G_{Oct-H_2O} = 27.69 \text{ kJ mol}^{-1}$ with an error below 0.10 kJ mol^{-1} resulting in a partition coefficient of $\log P_{Oct-H_2O} = 4.82 \pm 0.02$, less than 0.25 kJ mol^{-1} above the experimental value.^[1]



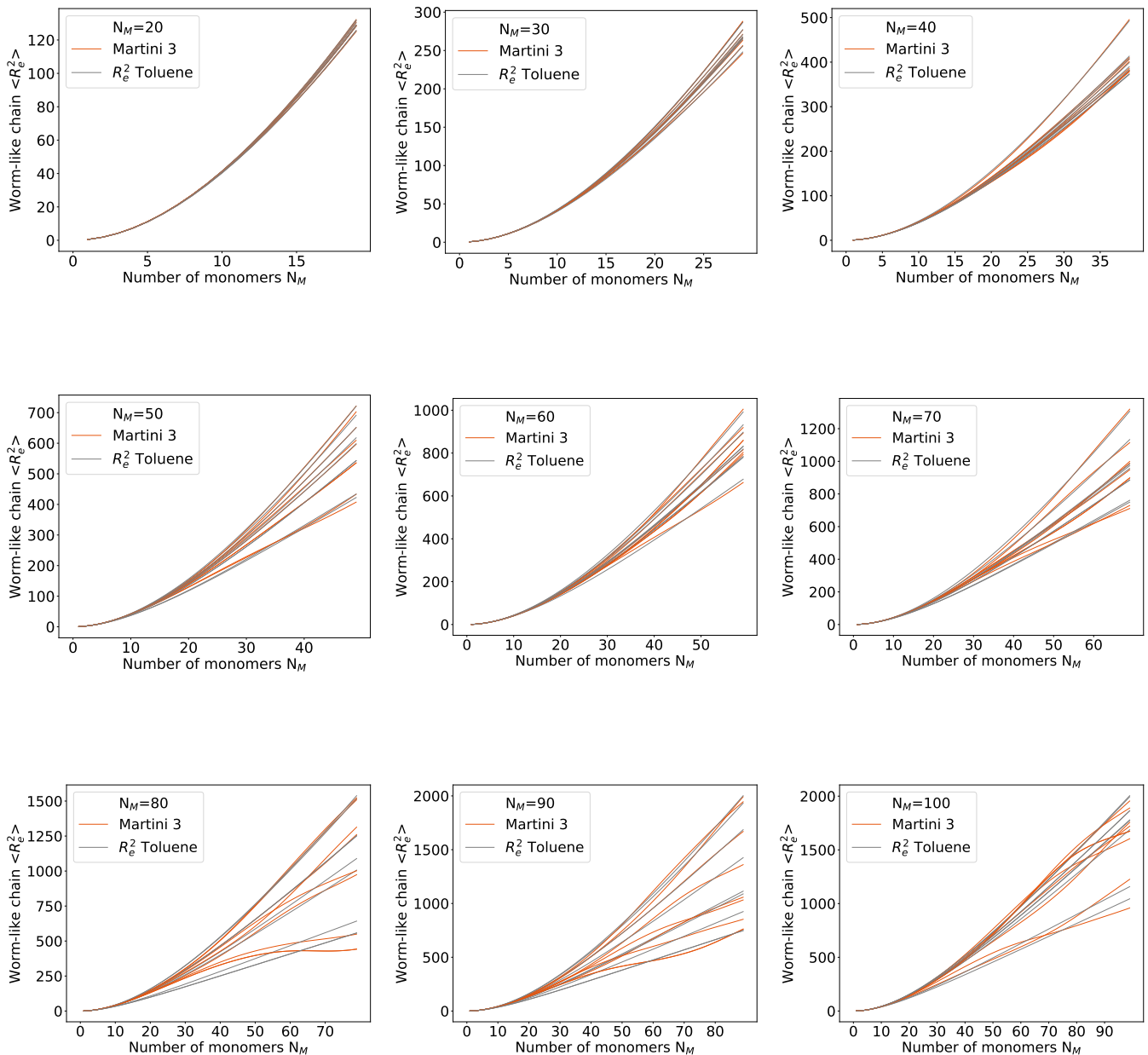
Supporting Figure 7 – Persistence length for PPE in water. Fitting the unit tangent vector auto correlation (eq.2) to a Martini 3 trajectory for a single 20 to 100 monomers long PPE chain in water.



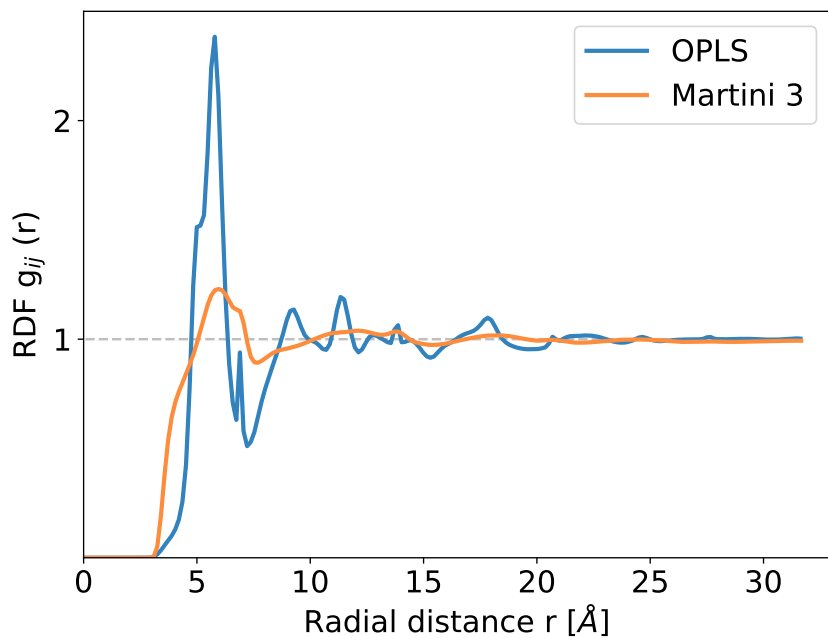
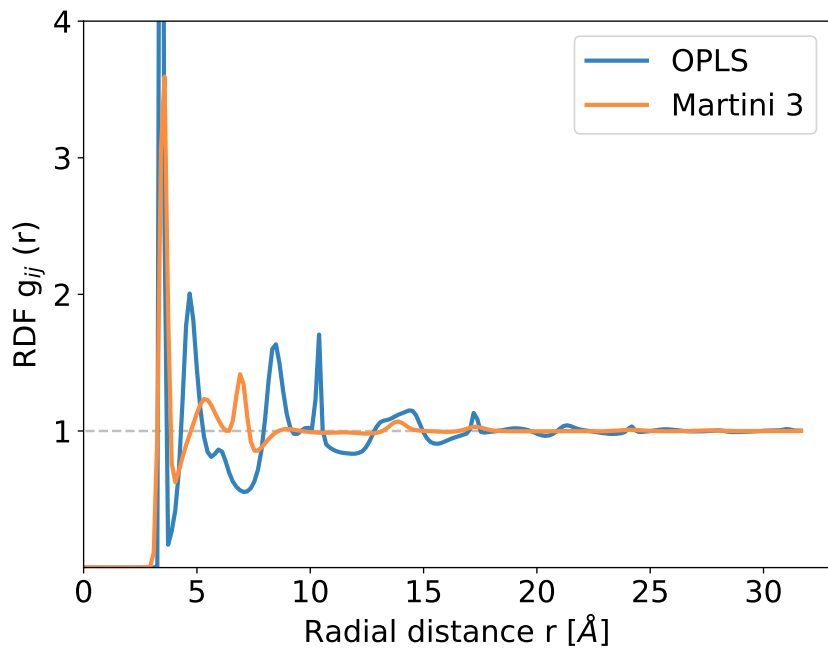
Supporting Figure 8 – Persistence length for PPE in water. Fitting the squared end-to-end distances from the worm-like chain theory (eq.3) to a Martini 3 trajectory for a single 20 to 100 monomers long PPE chain in water.



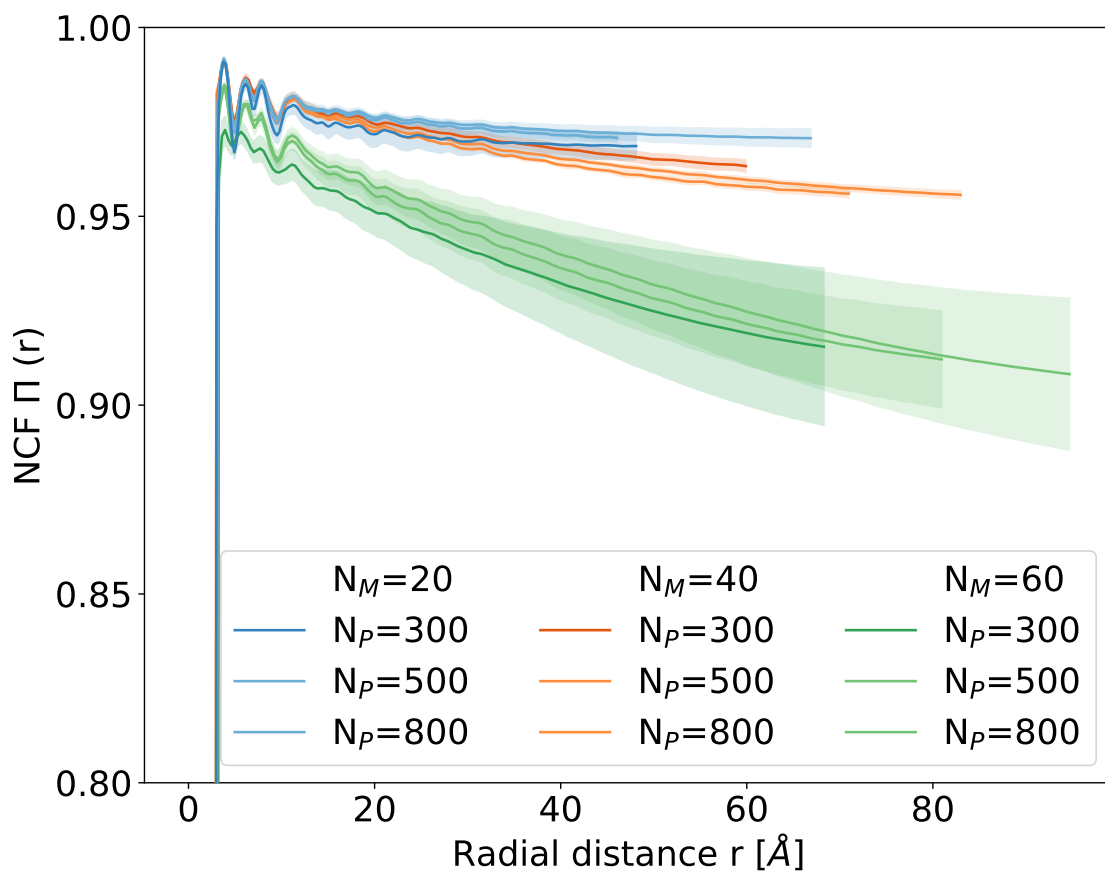
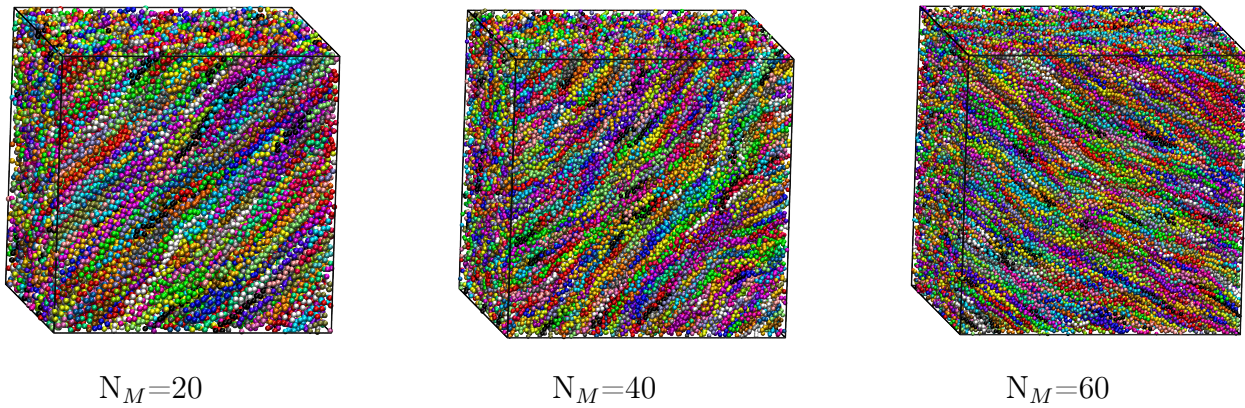
Supporting Figure 9 – Persistence length for PPE in toluene. Fitting the unit tangent vector auto correlation (eq.2) to a Martini 3 trajectory for a single 20 to 100 monomers long PPE chain in toluene.



Supporting Figure 10 – Persistence length for PPE in toluene. Fitting the squared end-to-end distances from the worm-like chain theory (eq.3) to a Martini 3 trajectory for a single 20 to 100 monomers long PPE chain in toluene.



Supporting Figure 11 – Packing in mid-size bulk systems. Comparing the RDF from mapped AA and CG simulations. We mapped the AA and CG trajectory to a one-bead-per aromatic ring and triple bond resolution (*above*) and to a one-bead-per triple bond resolution (*below*). For both cases, the mapped AA simulations show a higher local order than the mapped CG ones. Still, the CG model reproduces the first and second peak of the RDF.



Supporting Figure 12 – Alignment in large-scale annealed bulk systems. Snapshots from annealed bulk systems of 500 PPEs with lengths of 20, 40 or 60 monomers (*above*). We observe an overall very high degree of order (*below*). As expected and seen for the equilibrated bulk systems (Fig. 6), we find both a decrease in nematic alignment with increasing distance and a steady decay in ordering with increasing polymer chain length, independent of the box size.

References

1. Hansch, C., Leo, A., Hoekman, D. Exploring QSAR: Hydrophobic, electronic, steric constants. *ACS*. **1995**. ISBN 0841229937.
2. Cotts, P.M., Swager, T.M., Zhou, Q. Equilibrium Flexibility of a Rigid Linear Conjugated Polymer. *Macromolecules*. **1996**. 10.1021/ma9602583.
3. Kloppenburg, L., Jones, D., Claridge, J.B., Loya, H.C., Bunz, U.H.F. Poly(p-phenyleneethynylene)s Are Thermotropic Liquid Crystalline. *Macromolecules*. **1999**. 10.1021/MA990020P.
4. Ofer, D., Swager, T.M., Wrighton, M.S. Solid-State Ordering and Potential Dependence of Conductivity in Poly(2,5-dialkoxy-p-phenyleneethynylene). *Chem. Mat.* **1995**. 10.1021/cm00050a029.